

# Elucidation of the solution structure of cardiotoxin analogue V from the Taiwan cobra (*Naja naja atra*)— Identification of structural features important for the lethal action of snake venom cardiotoxins

GURUNATHAN JAYARAMAN,<sup>1,4</sup> THALLAMPURANAM KRISHNASWAMY SURESH KUMAR,<sup>1</sup>  
CHUNG-CHU TSAI,<sup>1</sup> SAMPATH SRISAILAM,<sup>1</sup> SHAN-HO CHOU,<sup>2</sup> CHEWN-LANG HO,<sup>3</sup>  
AND CHIN YU<sup>1</sup>

<sup>1</sup>Department of Chemistry, National Tsing Hua University, Hsinchu, Taiwan

<sup>2</sup>Institute of Biochemistry, National Chung-Hsing University, Taichung, Taiwan

<sup>3</sup>Institute of Biological Chemistry, Academia Sinica, Nankang, Taiwan

(RECEIVED November 3, 1999; FINAL REVISION January 28, 2000; ACCEPTED January 28, 2000)

## Abstract

The aim of the present study is to understand the structural features responsible for the lethal activity of snake venom cardiotoxins. Comparison of the lethal potency of the five cardiotoxin isoforms isolated from the venom of Taiwan cobra (*Naja naja atra*) reveals that the lethal potency of CTX I and CTX V are about twice of that exhibited by CTX II, CTX III, and CTX IV. In the present study, the solution structure of CTX V has been determined at high resolution using multidimensional proton NMR spectroscopy and dynamical simulated annealing techniques. Comparison of the high resolution solution structures of CTX V with that of CTX IV reveals that the secondary structural elements in both the toxin isoforms consist of a triple and double-stranded antiparallel  $\beta$ -sheet domains. Critical examination of the three-dimensional structure of CTX V shows that the residues at the tip of Loop III form a distinct “finger-shaped” projection comprising of nonpolar residues. The occurrence of the nonpolar “finger-shaped” projection leads to the formation of a prominent cleft between the residues located at the tip of Loops II and III. Interestingly, the occurrence of a backbone hydrogen bonding (Val27CO to Leu48NH) in CTX IV is found to distort the “finger-shaped” projection and consequently diminish the cleft formation at the tip of Loops II and III. Comparison of the solution structures and lethal potencies of other cardiotoxin isoforms isolated from the Taiwan cobra (*Naja naja atra*) venom shows that a strong correlation exists between the lethal potency and occurrence of the nonpolar “finger-shaped” projection at the tip of Loop III. Critical analysis of the structures of the various CTX isoforms from the Taiwan cobra suggest that the degree of exposure of the cationic charge (to the solvent) contributed by the invariant lysine residue at position 44 on the convex side of the CTX molecules could be another crucial factor governing their lethal potency.

**Keywords:** cardiotoxins; finger-shaped projection; lethal potency; receptor binding; solution structure

Snake venom cardiotoxins (CTXs) are small molecular weight (6.5–7.0 kDa), all  $\beta$ -sheet proteins, cross-linked by four disulfide bridges (Kumar et al., 1996a, 1997, 1998). Interestingly, cardiotoxins exhibit a wide variety of biological activities, which include contraction of cardiac muscles, lysis of erythrocytes, and selective killing of certain types of tumor cells (Harvey, 1985, 1991; Dufton & Hider, 1991). In addition, cardiotoxins are also reported to selectively inhibit key enzymes such as protein kinase C and Na<sup>+</sup>,

K<sup>+</sup>-ATPase (Chiou et al., 1995). However, to date, the exact molecular mechanism underlying the broad spectrum of biological activities exhibited by cardiotoxins is still an enigma.

Amino acid sequences of cardiotoxins isolated from various snake venom sources exhibit more than 90% sequence homology (Dufton & Hider, 1983; Sivaraman et al., 1997). Comparison of the three-dimensional (3D) structures of various cardiotoxin analogues reveals that the backbone folding of these toxin isoforms are mostly similar (Kumar et al., 1997). The secondary structural elements in this class of toxins are primarily  $\beta$ -sheets (Sivaraman et al., 1998a; Chang et al., 1998; Lee et al., 1998). Interestingly, despite the gross similarities in their 3D structures, snake venom cardiotoxins show significant difference(s) in their biological ac-

Reprint requests to: Chin Yu, National Tsing Hua University, Department of Chemistry, Hsinchu, Taiwan; e-mail: cyu@mx.nthu.edu.tw.

<sup>4</sup>Present address: Department of Life Sciences, National Tsing Hua University, Hsinchu, Taiwan.

tivities. This disparity in the biological activities is believed to stem from the subtle structural differences in the 3D structures of these toxins (Kumar et al., 1997).

To date, five different cardiotoxin isoforms have been isolated from the venom of the Taiwan cobra (*Naja naja atra*) (Sivaraman et al., 1997). Interestingly, the solution structures of four of these toxin isoforms [namely, CTX I (Jahnke et al., 1994), CTX II (Bhaskaran et al., 1994a), CTX III (Bhaskaran et al., 1994b; Sivaraman et al., 1998b), and CTX IV (Jang et al., 1997)] have recently been solved. Cardiotoxin analogue V (CTX V) was recently isolated and chemically characterized (Chiou et al., 1995; Sivaraman et al., 1997). In the present study, we have determined the solution structure of CTX V from the Taiwan cobra using 2D and 3D proton NMR spectroscopy. To understand the molecular basis of the lethal action(s) of cardiotoxins, we compare the lethal potency and 3D structure(s) of CTX V with other the cardiotoxin isoforms from the Taiwan cobra venom. Careful analysis of the 3D structures (of the cardiotoxin isoforms) in conjunction with the available data in the literature on the structure-function relationship of snake venom cardiotoxins clearly suggest that the lethal potency of cardiotoxins is strongly dependent on the presence of a well-defined nonpolar "finger-shaped" projection on the convex side and the occurrence of a prominent cleft between the residues located at the tip of Loops II and III of the cardiotoxin molecule. This study for the first time hints at the possibility of cardiotoxins exerting their biological action(s) by specifically binding to definite cell surface receptors.

## Results and discussion

Five cardiotoxin isoforms have so far been isolated from the venom of the Taiwan cobra (*Naja naja atra*) (Fig. 1; Sivaraman et al., 1997). There exists more than 90% homology in the amino acid sequence of these cardiotoxin isoforms (Fig. 2). It is important and interesting to understand the structure-function relationships that possibly exist among these cardiotoxin isoforms. It is in this context that the present study is aimed at understanding the structural basis for the difference(s) in the lethal potencies of the five cardiotoxin analogues isolated from the same venom source (*Naja naja atra*).

### Lethal potency

The lethal potency of the various cardiotoxin isoforms is given in Figure 3A. It could be visualized that the lethal potency of CTX I and CTX V is about half that of the other cardiotoxin isoforms isolated from the Taiwan cobra. At a dosage of  $1.5 \mu\text{g/g}$  of mouse, the lethal potency of CTX I and CTX V is  $6.0 \pm 0.6$  and  $8.6 \pm 0.3$  min, respectively (Fig. 3A). At the same toxin dose ( $1.5 \mu\text{g/g}$  of mouse), CTX II, CTX III, and CTX IV are found to be less toxic (Fig. 3A). CTX IV is found to be the least potent of the cardiotoxin isoforms with a lethal potency of  $26.8 \pm 0.68$  min. Estimation of the  $\text{LD}_{50}$  values of the five cardiotoxin isoforms from the Taiwan cobra bears a good correlation with their estimated lethal potency (Fig. 3B). These results clearly demonstrate that despite the high

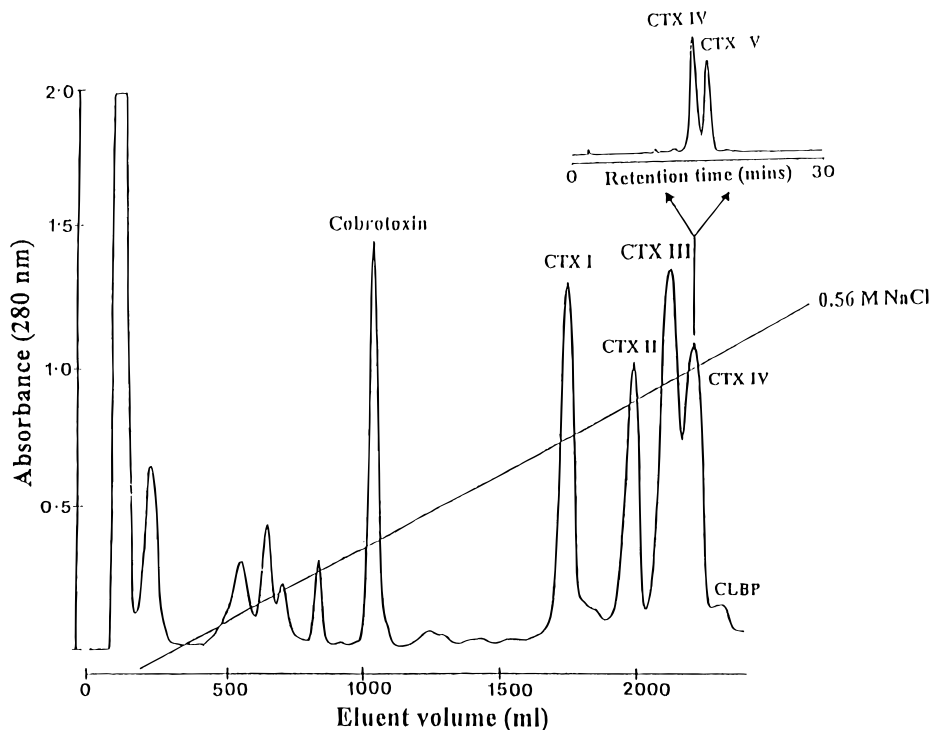


**Fig. 1.** Fractionation profile of the crude Taiwan cobra (*Naja naja atra*) venom on a cation exchanger (SP-Sephadex C-25). The elution of the protein components was carried out using a linear NaCl gradient (0–5.6 M) in 0.025 M phosphate buffer (pH 7.5). The last fraction (inner peak) noticed in the elution profile represents the "cardiotoxin like-basic protein (CLBP)." The inset figure represents the two components (CTX IV and CTX V) obtained by fractionation of the peak IV on a reversed-phase ( $\text{C}_{18}$ ) HPLC column, using a linear water-acetonitrile gradient. The elution of proteins was monitored by the 280 absorbance.

CTX I	LKCNKLIPIA	SKTCPAGKNL	CYKMFMSDL	TIPVKRGCID	VCPKNSLLVK	YVCCNTDRCN
CTX II	LKCNKLVPLF	YKTCPAGKNL	CYKMFVSNL	TVPVKRGCID	VCPKNSALVK	YVCCNTDRCN
CTX III	LKCNKLVPLF	YKTCPAGKNL	CYKMFVATP	KVPVKRGCID	VCPKSLLVK	YVCCNTDRCN
CTX IV	RKCNKLVPLF	YKTCPAGKNL	CYKMFVSNL	TVPVKRGCID	VCPKNSALVK	YVCCNTDRCN
CTX V	LKCNKLVPLF	YKTCPAGKNL	CYKMFVSNK	MVPVKRGCID	VCPKSLLVK	YVCCNTDRCN

Fig. 2. Amino acid sequence of the five cardiotoxin isoforms isolated from the Taiwan cobra (*Naja naja atra*) venom (from Kumar et al., 1997).

degree of homology (<90%) in their amino acid sequence, cardiotoxin isoforms could indeed significantly differ in their lethal potency.

#### NMR assignments and structure description of CTX V

Assignments of nearly all proton resonances of CTX V were achieved using the information obtained from the double-quantum filter correlation spectroscopy (DQF-COSY), total correlation spectroscopy (TOCSY), and nuclear Overhauser effect spectroscopy (NOESY) spectra of the protein (Wuthrich, 1986). The four proline residues were unambiguously identified from their J-connectivity network in the TOCSY and the NOESY spectra (data not shown). The NOEs of  $\text{NH}_{i-1}$ - $\text{ProH}_i^{\delta}$  indicate a "trans" conformation for the proline residues in the toxin. The assignments made from the 2D-homonuclear experiments were verified critically by performing the 3D NOESY-TOCSY experiment. The minor ambiguities, which existed in the assignment of the proton resonances in the 2D-NMR, were resolved using the NOESY-TOCSY spectrum. Figure 4 shows the NOESY plane of the protons that constitute Strand IV (residues 35 to 40) of CTX V. The strips indicate the sequential NOE connectivities observed for the amide protons of Lys35-Asp40. Using the main-chain directed (MCD) strategy, the secondary structural elements in the toxin are found to be primarily  $\beta$ -sheets. The residues Lys2-Lys5, Tyr1-Cys14, Leu20-Phe25, Val34-Ile39, and Lys50-Cys55 comprise the five  $\beta$ -strands I to V, respectively.  $\beta$ -Strands I and II constitute the antiparallel double-stranded  $\beta$ -sheet segment and the  $\beta$ -strands III, IV, and V comprise the triple stranded  $\beta$ -sheet domain. The structure of CTX V was calculated based on a total of 504 distance constraints. The overlap of the simulated annealing structures is in

good agreement with the NMR data. The backbone root-mean-square deviation (RMSD) values in CTX V is 0.68 Å (Table 1). Considering the well-defined secondary structural regions and excluding the more disordered loops, the backbone RMSD is in the range of 0.19–0.28 Å. Convergence of the selected structures was also confirmed by the  $\varphi$  and  $\psi$  values and are found to be within their allowed region(s). Thus, based on the structural statistics on CTX V, it is obvious that the solution structure of CTX V is at high resolution, and hence meaningful and reliable conclusions on the structure-function relationship could be derived based on its (CTX V) structure. The authenticity of the calculated structures was also cross-checked by back-calculating the NOESY spectrum from the

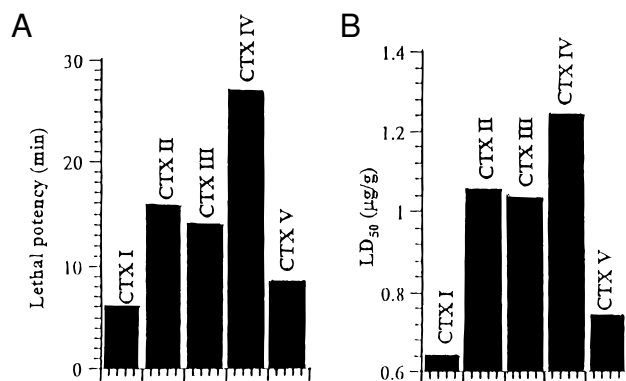


Fig. 3. Comparison of the (A) lethal potency and (B) LD<sub>50</sub> values of various isoforms of cardiotoxin isolated from the Taiwan cobra (*Naja naja atra*) venom.

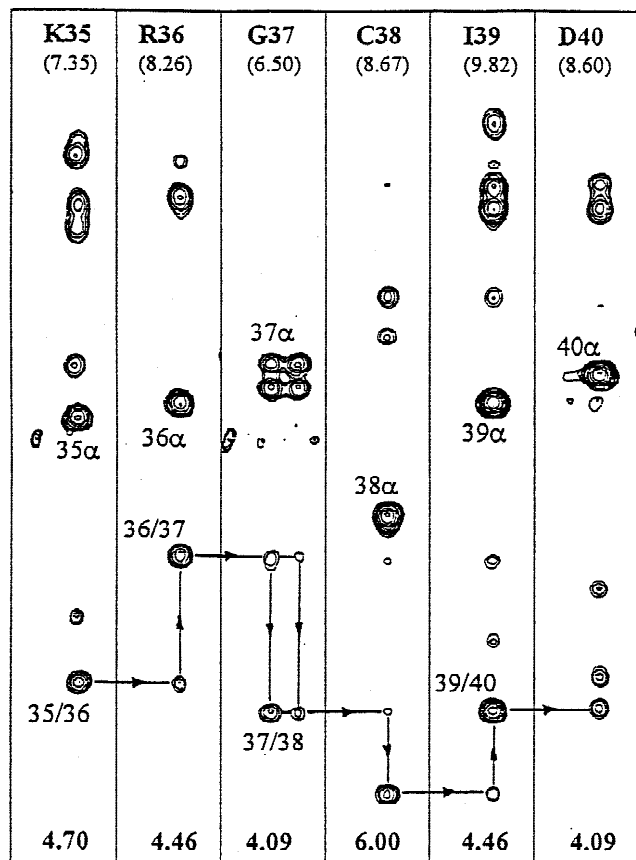


Fig. 4. Sequential NOE connectivities of the residues Lys35-Asp40 as observed from the 3D NOESY-TOCSY spectra of CTX V. The numbers depicted at the bottom of each strip represents the alpha proton chemical shifts (in F2 dimension) of the corresponding residues. The numbers indicated in parentheses (in the top portion of each strip) are the amide proton chemical shifts in the F3 dimension.

**Table 1.** Structural statistics for the calculated solution structures of CTX V from the Taiwan Cobra (*Naja naja atra*) venom

Constraints used in the calculation	
Long-range distance restraints	149
Sequential distance restraints	164
Intraresidual distance restraints	161
Disulfide distance restraints	4
Hydrogen bond restraints	26
Backbone dihedral angle restraints	46
Side-chain stereospecific restraints	16
Energetics of the final structures (Explicit X-PLOR terms)	
Overall energy	151.8
NOE energy	8.3
VDW energy	9.9
CDIH energy	1.2
RMSDs from the covalent geometry	
Bond length	0.002
Bond angle	0.649
Impropers	0.395
RMSDs of the calculated structures	
Backbone atoms (residues 1–60)	0.68
Double stranded $\beta$ -sheet (residues 2–5 and 11–14)	0.19
Triple stranded $\beta$ -sheet (residues 20–25, 34–39, and 50–55)	0.28

X-PLOR derived CTX V solution structures. The experimental and back-calculated spectra bear a good resemblance to each other (data not shown), implying that the resonance assignments and the distance constraints utilized in the calculation of the structure of CTX V are reasonably accurate.

#### Description of the solution structure of CTX V

The solution structure of CTX V reveals that it is a “three-finger” shaped protein with three loops emerging from a globular head (Fig. 5). The secondary structure of the toxin (CTX V) is exclusively  $\beta$ -sheet, comprising of five strands protruding from a globular head. The five  $\beta$ -strands are found to align themselves antiparallelly into double- and triple-stranded  $\beta$ -sheets (Fig. 5). The head region of the molecule is extensively cross-linked by four disulfide bridges. The high density of the disulfide links found in the core region of the molecule is known to contribute significantly to the stability of the cardiotoxin molecule.

Loop I in the CTX V molecule comprises of residues 2 to 14 and is lodged in the double-stranded  $\beta$ -sheet segment. Residues in this loop (Loop I) are believed to be important for the erythrocyte lytic activity (Gantineau et al., 1987; Kini & Evans, 1989; Menez et al., 1990; Menez et al., 1992). The extremity of Loop I from Leu6 to Tyr11 is completely hydrophobic and is encircled by basic residues such as Lys2, Lys5, and Lys12. Comparison of the amino acid sequences of various cardiotoxin analogues reveal that these residues comprising the hydrophobic patch are either invariant and/or mutable only to other hydrophobic side chains. This stretch of apolar residues in Loop I is predicted to be important for the erythrocyte activity of the cardiotoxins (Dufton & Hider, 1991). Loop II of the CTX V molecule consists of the  $\beta$ -sheet secondary structure between residues 20 to 25 and 35 to 39. The characteristic  $\beta$ -bulge found in other cardiotoxin analogues, such as CTX III and CTX IV (Jang et al., 1997), is found missing in CTX V. As a consequence, the prominent twist in the triple-stranded  $\beta$ -sheet found in the solution structure of CTX III and CTX IV is absent in CTX V. In CTX V, the residues constituting the triple-stranded  $\beta$ -sheet segment are in the same plane. The residues at the tip of Loop II in CTX V are found to be highly flexible. The polypeptide chain from Loop II in CTX V crosses over to other side of the

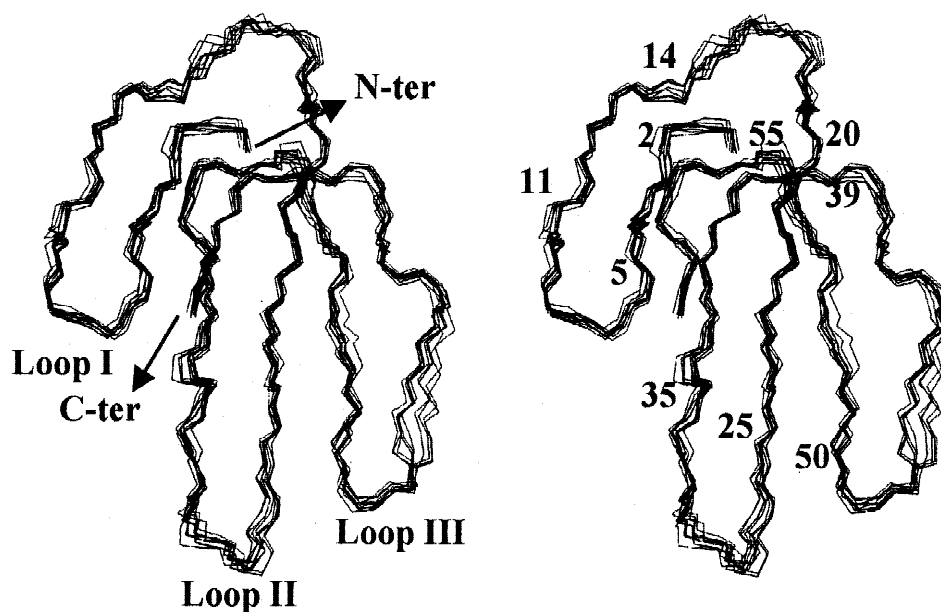


**Fig. 5.** Stereoview of the best-fit superposition of the 14 NMR solution structures of CTX V as determined by dynamical simulated annealing calculations. The residue numbers indicate the location of each of the  $\beta$ -strands that make up the double- and triple-stranded  $\beta$ -sheet segments in the toxin.

protein to constitute the first half of Loop III and makes a well-defined type I  $\beta$ -turn between residues 46 and 49. The Loop III is completed by an extended segment between the residues 50 and 55 that antiparallels residues 20 to 25 to form the triple stranded  $\beta$ -sheet. Similar to the solution structures of other cardiotoxin analogues, CTX V presents many sites of contact between the N- and the C-terminal ends, thereby bringing them topologically proximal to each other (Jang et al., 1997). The N- and C-termini are connected by hydrogen bonds between Arg58NH and Lys2CO as well as between Asn4NH and Asn60CO. These four residues are well conserved among all the cardiotoxin sequences.

#### Comparison of the three-dimensional structures of CTX V and CTX IV

It is important to understand the structural basis for the observed difference(s) in the lethal potency of the various cardiotoxins isolated from the Taiwan cobra venom. The 3D structure of CTX IV was recently determined at high resolution (Jang et al., 1997). In addition, among the cardiotoxin analogues isolated from the Taiwan cobra venom, the lethal potency and LD<sub>50</sub> values are the least for CTX IV. As the solution structures of CTX IV and CTX V are at high resolution and also their lethal potency are drastically different, comparison of the 3D structures of these two cardiotoxin isoforms would provide useful insights into the structural determinants responsible for the differences in the lethality of the toxin isoforms from a single venom source (*Naja naja atra*).

CTX IV isolated from the Taiwan cobra differs in the amino acid sequence of CTX V at five positions. Leu1, Lys30, Met31, Ser45, and Leu47 in CTX V are replaced by Arg, Leu, Thr, Asn, and Ala, respectively, in the corresponding positions in the amino acid sequence of CTX IV (Fig. 2). Comparison of the solution structures of CTX V and CTX IV reveals that the two toxin analogues possess grossly similar 3D structures. In fact, the residues constituting the double- and triple-stranded  $\beta$ -sheet segments are identical.

The organization of the side chains in the 3D structures of cardiotoxins is known to give rise to two different surfaces (concave and convex) with well-defined properties. Comparison of the structural interactions present on the concave surface in both CTX V and CTX IV reveals no prominent differences. The convex surface in both in CTX IV and CTX V contains a large hydrophobic patch contributed by residues located in the three loops. The hydrophobic patch consists of about 10 residues located in two clusters. In both the toxin isoforms (CTX IV and CTX V), the hydrophobic clusters are organized around two tyrosine residues (Tyr22 and Tyr51). Results based on chemical modification studies revealed that Tyr22 and Tyr51 play a crucial role in the maintenance of the 3D structure(s) of cardiotoxins (Gantineau et al., 1987). In both the toxin isoforms (CTX IV and CTX V), the hydrophobic patch is surrounded by a group of three basic residues namely, Lys12, Lys18, and Lys35 (Kini & Evans, 1989). Systematic chemical modification studies by Menez et al. (1990, 1992) revealed that these cationic residues are intricately involved in the erythrocyte lytic activity of snake venom cardiotoxins. The results presented thus far clearly show that most of the structural interactions in the concave and convex sides are identical and cannot account for the observed difference(s) in the lethal potency of CTX IV and CTX V.

#### Formation of a nonpolar "finger-shaped" projection on the convex surface

It has been proposed that residues located at the tip of Loop III play an important role in the lethal activity of snake venom cardiotoxins (Dufton & Hider, 1983). Critical comparison of the solution structures of CTX IV and CTX V on the convex surface reveals significant differences in the orientation of the residues located at the tip of Loop III in these two toxin (CTX IV and CTX V) analogues (Fig. 6). A type I  $\beta$ -turn between residues 46 and 49 is found to occur consistently in the three-dimensional structures

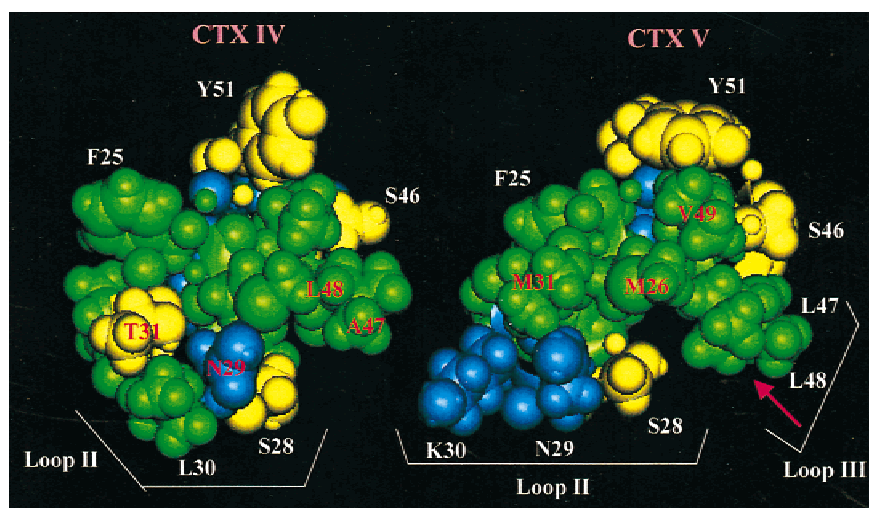


**Fig. 6.** Graphical representation of the topology of the residues at the tip of Loops II and III in the 3D solution structures of CTX IV and CTX V. It could be deduced that a distinct nonpolar finger-shaped projection (indicated by a red arrow) comprising of the hydrophobic residues (green) (Leu47 and Leu48) is formed at the tip of Loop III in CTX V. It is predicted that this finger-shaped projection could constitute a portion of the putative receptor binding site of cardiotoxins. The polar residues are represented in yellow and the positively charged and amide side chains are indicated in blue.

of all the snake cardiotoxins. The structural or functional importance of the existence of these  $\beta$ -turns has yet not been identified. The presence of the type I  $\beta$ -turn in CTX V is responsible for the orientation of the nonpolar side chains of Leu47 and Leu48 as a "finger-shaped" projection at the tip of Loop III on the convex side of the molecule. This nonpolar finger-shaped projection could probably constitute a portion of the putative receptor binding site. Interestingly, despite the presence of the conserved type I  $\beta$ -turn between Ser46 and Val49 in CTX IV, the nonpolar residues (Ala47 and Leu48) at the tip of Loop III do not clearly emerge out as a finger-shaped projection on the convex surface (Fig. 6).

It is important to analyze the reason(s) as to why the residues at the tip of Loop III in CTX IV do not protrude out on the convex side of the toxin molecule. Careful scrutiny of the interactions among the residues located at the tip of Loop III in CTX IV shows that Leu48NH is hydrogen bonded to Val27CO (Fig. 7, indicated by an arrow). The solution structure of CTX V shows the absence of this hydrogen bond (between Val27CO and Leu48NH). The presence of this hydrogen bond between residues located at the tip of Loops II and III is found to distort the backbone conformation at the tip of Loop III and consequently positions this loop (Loop III) spatially closer to the tip of Loop II. The net result is that the side chains of the nonpolar residues (Ala47 and Leu48) fail to loop out as a finger-shaped projection (at the tip of Loop III) as observed in the solution structure of CTX V. In addition, the relatively smaller side chain of Ala47 also appears to be responsible for the lack of a prominent projection on the convex side of the CTX IV molecule. It is pertinent to mention that the presence of a hydrogen bond between Val27CO and Leu48NH in CTX IV (Fig. 7) also appears to effect the hydrophobic cluster at the tip of Loops II and III. This could be evidenced from the differences in the amide proton chemical shifts of residues such as Phe25, Met26, Ser46, and Tyr51 in CTX IV and CTX V, respectively (Fig. 8).

#### Formation of the cleft enclosed between Loops II and III

There are two well-conserved methionine residues (Met24 and Met26) in the cardiotoxin isoforms isolated from various snake venom sources. Chemical modification studies have unambiguously indicated that one or both of these methionine residues are

crucial for the lethality of the snake venom cardiotoxins (Dufton & Hider, 1991). Carlsson and Louw (1978) studying the role of methionine residues in the lethal activity of cardiotoxin V<sup>H1</sup> from *Naja melanoleuca* showed that chemical modification of the methionine residues resulted in substantial (>80%) loss in the lethal activity of the toxin (cardiotoxin). It was suggested that the more solvent exposed of the two methionine residues, Met26, is important for the lethal action of the snake venom cardiotoxins. Comparison of the solution structures of CTX IV and CTX V reveals a significant difference in the degree of exposure of Met26. Owing to the orientation of the nonpolar side chains of Leu47 and Leu48 into a finger-shaped projection on the convex surface, a prominent cleft is formed between the residues located at the tip of Loops II and III in the CTX V molecule (Fig. 6). This structural feature in CTX V increases the degree of exposure of Met26 on the convex surface of the toxin molecule and probably enhances the affinity of the toxin to the receptor. However, in CTX IV, the hydrogen bond between Val27CO and Leu48NH forces the residues located at the tip of Loops II and III to move spatially closer. This aspect reduces the size of the cleft formed between the tip of Loops II and III (Figs. 6, 7). The net consequence of this conformational topology is the decreased solvent exposure of Met26 in CTX IV. It is probable that the lower degree of solvent exposure of the thioether side chain of Met26 results in weaker toxin-receptor interaction(s) and consequently accounts for the weaker lethal potency of CTX IV.

#### Differential orientation of the side chain of Lys44

There are two lysine residues at positions 44 and 50 in the amino acid sequences of CTX IV and CTX V. Lys44 is almost invariably present in the amino acid sequences of all cardiotoxins. Chemical modification of Lys44 has been shown to result in substantial loss in the lethal potency of a cardiotoxin analogue from *Naja nigricollis* (Hodges et al., 1987; Menez et al., 1990). Shashidharan and Ramachandran (1987), based on chemical modification studies on cardiotoxin analogue I from Indian cobra (*Naja naja naja*), demonstrated that modification of lysine residues in Loops I and II resulted in substantial loss in the erythrocyte lytic activity of the cardiotoxin analogue but its lethal potency remained unperturbed. However, modification of lysine residues in Loop III (including

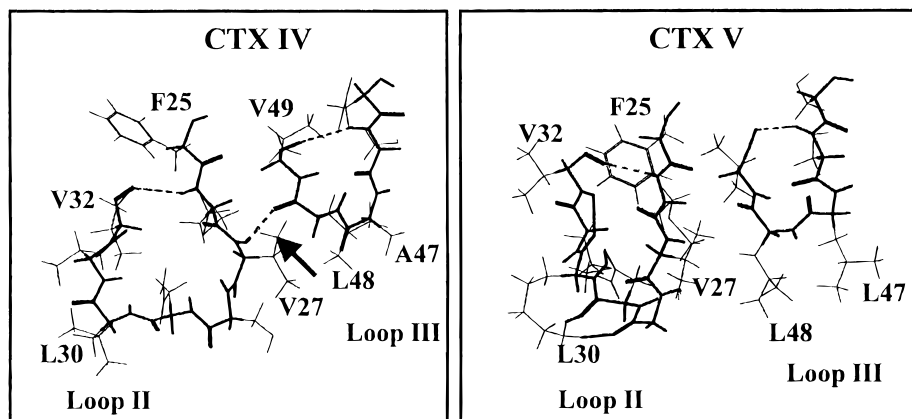


**Fig. 7.** Depiction of the structural interactions among the residues at the tip of Loops II and III. Hydrogen bonds among residues located at the distal portion of Loops II and III are indicated by dotted lines. The arrow in the structure of CTX IV indicates the hydrogen bond between Val27CO and Leu48NH. This hydrogen bond is absent in CTX V.

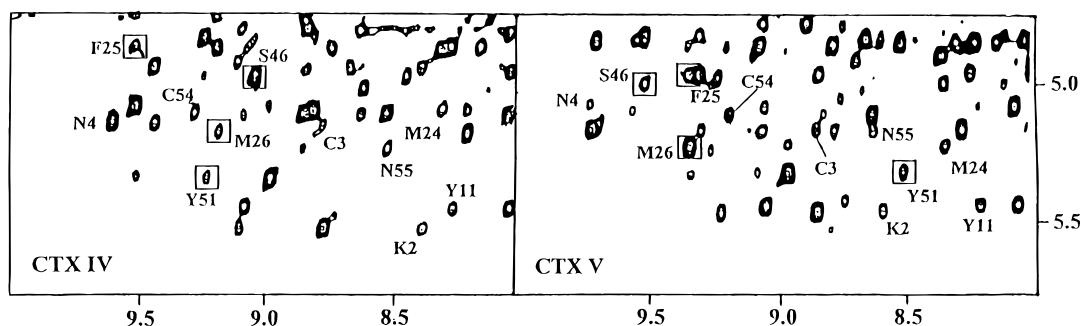


**Fig. 8.** Representation of the cross peaks in the fingerprint region (NH-C $\alpha$ H) region of the NOESY spectra of CTX IV and CTX V. The differences in the orientation of residues involved at the tip of Loops II and III are manifested in the chemical shifts of the residues in these toxin isoforms. For example, the amide proton resonances of F25, M26, S46, and Y51 in CTX V (labeled within a square) are different from those observed for the same residues in CTX IV.

Lys44) was reported to result in significant loss in the lethal activity of the cardiotoxin analogue (Shashidharan & Ramachandran, 1987). Thus, based on the results of these studies, it appears that the conserved lysine residue at position 44 in Loop III is important for the lethal activity of snake venom cardiotoxins. Comparison of the solution structures of both CTX V and CTX IV reveals that the orientation of the side chain of Lys44 is different in these toxin isoforms (Fig. 9). Most portions of the positively charged side chain of Lys44 are projected on the convex side of the CTX V molecule. However, in CTX IV, the side chain of Lys44 are found to be projected on the concave side (Fig. 9). This reversal in the direction of orientation of the positively charged side chain of Lys44 appears to influence the lethal activity of snake venom cardiotoxins.

#### Comparison with the 3D structures of other cardiotoxin isoforms

Availability of the solution structure data on all the five cardiotoxin isoforms in the Taiwan cobra (*Naja naja atra*) venom serves as an incentive to understand the structural determinants responsible for the lethal potency of cardiotoxin isoforms isolated from the same venom source. Comparison of the solution structures of CTX V individually with those of CTX I, CTX II, CTX III, and CTX IV reveals interesting differences (Fig. 9). The solution structures of CTX I and CTX V share many similarities. Just as in CTX V, the 3D structure of CTX I shows a well-defined finger-shaped projection comprising of the nonpolar side chains of Leu47 and Leu48 (Fig. 6). Interestingly, the structure of CTX I depicts a striking resemblance with that of CTX V in possessing a prominent cleft (at the tip of Loops II and III) that increases the solvent exposure of the functionally important side chain of Met26. In addition, the solution structure of CTX I shows a higher degree of exposure of the side chain of Lys44 on the convex surface of the molecule (Fig. 9). The marginally higher lethal potency exhibited by CTX I (as compared to CTX V) could be due to the greater exposure of the cationic charge on the side chain of Lys44 on the convex surface of the molecule (Fig. 9). Thus, it is interesting to note that CTX I and CTX V, which exhibit higher lethal potency, show striking conformational similarities at the putative functional site (at the tip of Loops II and III).

CTX III, like CTX I and CTX V, possesses a leucine at position 47 and lacks the hydrogen bond between Val27CO and

Leu48NH. However, unlike CTX I and CTX V, the nonpolar finger-shaped projection and the cleft formed at the tip of Loops II and III are not very prominent as observed in the average structure of CTX III. This is due to the presence of proline at position 30 (located at the distal end of Loop II), which introduces a twist in the backbone of the toxin (CTX III) molecule. As a consequence, the tip of Loop II moves spatially closer to the residues located at the tip of Loop III. This aspect decreases the size of the cleft (and thereby the solvent exposure of Met26). The movement of the residues located at the distal ends of Loops II and III also causes a “leveling effect” wherein the finger-shaped projection is not prominently observed. In addition, it could be noticed that the extent of exposure (on the convex surface of the molecule) of the side chain of the functionally important Lys44 is significantly lesser than that observed in CTX I and CTX V. These structural features probably account for the lower lethal potency of CTX III as compared to that of CTX I and CTX V.

CTX II and CTX IV contain an Ala47 instead of a leucine residue in that position in CTX I, CTX III, and CTX V. The 3D structure of CTX II shows a hydrogen bond between Val27CO and Leu48NH. As described earlier, this hydrogen bond is responsible for the close packing of the residues located at the tips of Loops II and III. The prominent cleft observed in the structures of CTX I and CTX V is also found lacking in CTX II. It appears that the occurrence of a hydrogen bond tethering the residues at the tip of Loops II and III and the presence of a less bulkier side chain of Ala47 accounts for the lack of the prominent nonpolar finger-shaped projection at the tip of Loop III in CTX II. Interestingly, it could be observed that the side chain of Lys44 (Fig. 9) is projected on the concave surface instead of the convex surface (as observed in the solution structures of CTX I, CTX III, and CTX V). These structural features are probably responsible for the weaker lethal potency of CTX II.

#### Is there a receptor for snake venom cardiotoxins?

Critical comparison of the lethal potency and 3D structures of the cardiotoxin isoforms suggest that three structural features could be crucial for the lethality of snake venom cardiotoxins. They are: (1) the presence of a nonpolar finger-shaped projection at the tip of Loop III, (2) occurrence of a prominent cleft between residues at the tip of Loops II and III, and (3) the degree of exposure of the cationic charge contributed by Lys44 on the convex surface of the

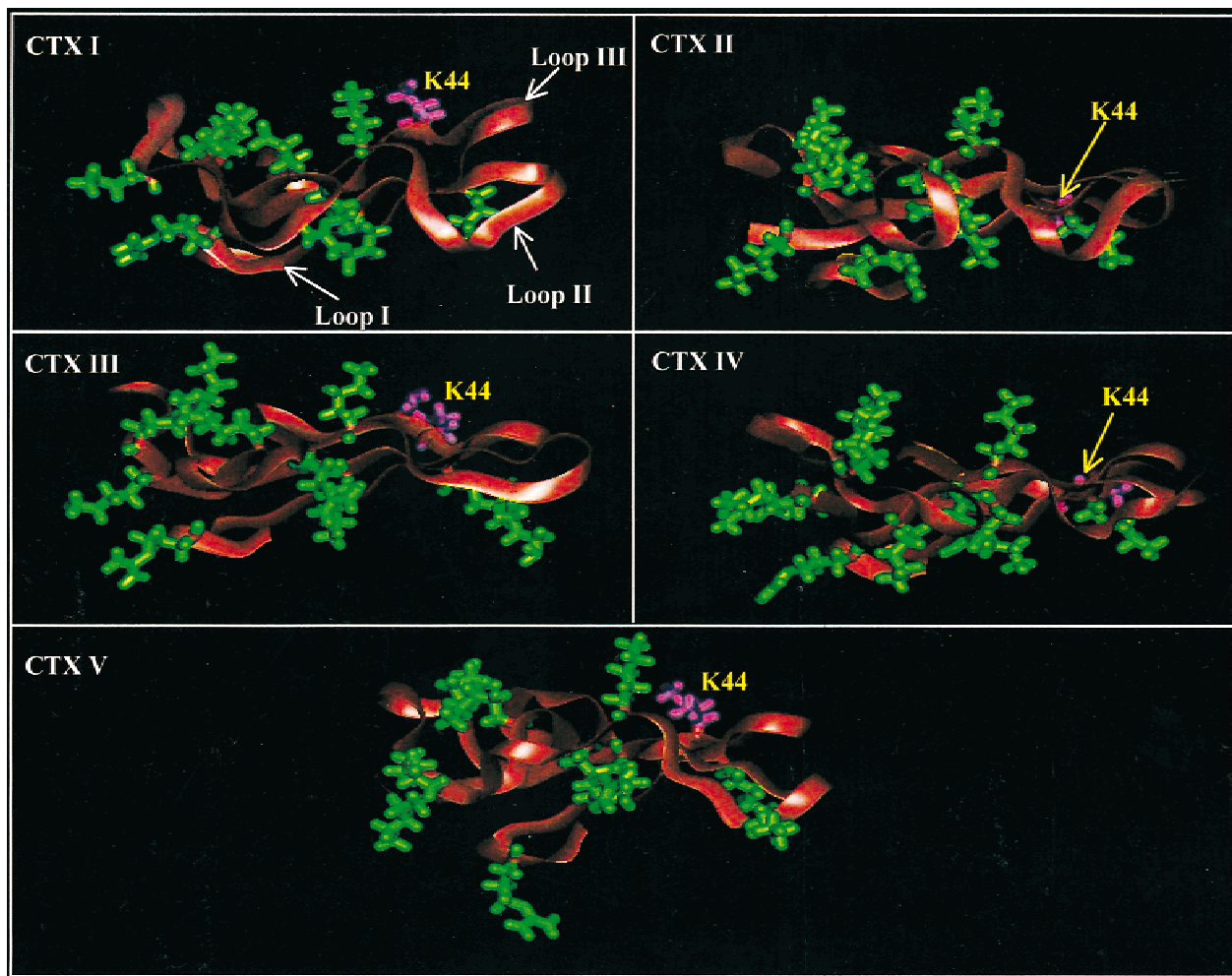


**Fig. 9.** Comparison of the distribution of the positively charged (lysine and arginine) residues in the various cardiotoxin (I–V) analogues. The differential orientation of the positively charged side-chain group of the invariant Lys44 is contemplated to play a crucial role in the lethal potency of the cardiotoxin isoforms. The side chain of Lys44 (indicated in violet) is projected on the convex side in CTX I, CTX III, and CTX V. However, in CTX IV and CTX II, the side-chain Lys44 is oriented toward the concave side of the molecule. For accurate representation of the orientation of the side chains in the various cardiotoxin isoforms, the backbone of the average structures (of the cardiotoxin isoforms) was optimally overlapped and later tilted orthogonally such that the convex surface in all the cardiotoxin isoforms project upward.

molecule. The results obtained in the present study hint at the possibility of the presence of a cell membrane specific receptor(s) for cardiotoxins, wherein the cardiotoxin molecules exert their defined action(s) on the target tissue by binding to the “receptor” in a lock-and-key mechanism. Although, to date, no clear model exists to explain the molecular basis for the lethal activity of cardiotoxins, there are reports in the literature suggesting the possibility of specific cellular receptors for cardiotoxins. Thelestam and Mollby (1979) investigating the binding of various cell types to cardiotoxins demonstrated the existence of receptor proteins on human fibroblast cell surface that bind specifically to snake venom cardiotoxins. Similarly, Takechi et al. (1985, 1986) and Condrea (1974) independently demonstrated the existence of specific high affinity receptors on the surface erythrocytes and certain muscle preparations. It would be of interest to note that Shiau Lin et al. (1976), using radiolabeled cardiotoxin analogues from the Taiwan cobra (*Naja naja atra*), unambiguously demonstrated the existence

of high affinity receptor binding sites on chick *biventer cerevicis* muscle. Similarly, recently Rees and Bilwes (1993), attempting to rationalize the multitude of biological properties through a common mechanism, suggested the possibility of the existence of definite cellular receptors for snake venom cardiotoxins. In the context of the increasingly accumulating evidence for the possibility of existence of specific cardiotoxin receptors, the identification of a distinct, finger-shaped projection architecture assumed by residues located at the tip of Loop III bears considerable significance. Since the lethal potency of the cardiotoxin analogue is strongly influenced by the presence/absence of this structural (finger-shaped projection) geometry, it would not be far-fetched to contemplate that the residues at the tip of Loops II and III are intricately involved in the binding of the toxin to the putative receptor. However, it should be mentioned that based on the results obtained in the present study, it is difficult to make a judgment whether the residues at the tip of Loops II and III are solely involved in the

proposed "receptor binding" or the residues in Loop I in the cardiotoxin molecule also have a role to play in the receptor binding.

Recently, the cloning and expression of CTX III from the Taiwan cobra (*Naja naja atra*) have been successfully achieved (Kumar et al., 1996b). In this context, using site-specific mutants of CTX III, it should be possible to delineate the structural constituents of the cardiotoxin receptor binding site.

## Materials and methods

Cardiotoxin isoforms (CTX I, CTX II, CTX III, CTX IV, and CTX V) were isolated from the crude venom (Sigma, St. Louis, Missouri) of the Taiwan cobra (*Naja naja atra*) using the SP-Sephadex C-25 as per the procedure of Yang et al. (1981) and purified further using the reversed-phase C<sub>18</sub> semipreparative high-performance liquid chromatography (HPLC) column. The authenticity of the protein sample was confirmed by performing the amino acid composition analysis and FAB mass.

### Estimation of the LD<sub>50</sub> value and lethal potency

The dosage required to kill 50% of mice in an experiment (LD<sub>50</sub>) of the five cardiotoxin (isolated from the Taiwan cobra) isoforms were measured by intravenous injection of the sample into the tail vein of the experimental mice (~20 g). Six mice were used in each dosage (at a CTX concentration of 15 µg/g of mice). Six control mice were treated under the same conditions, but without the CTX samples. The toxicity was also expressed as lethal potency that is defined as the time elapsed for mice to reach death after intravenous injection of a fixed concentration of CTXs. In all cases, the toxins were dissolved in buffered saline.

### NMR data collection and structure calculation

Proton NMR experiments were recorded for the CTX V (5 mM) sample in 95% H<sub>2</sub>O/5% D<sub>2</sub>O solvent mixture. DQF-COSY (Rance et al., 1983), TOCSY (mixing period of 80 ms; Bax & Davies, 1985), and water-gated NOESY (Piotto et al., 1992) experiments (mixing times of 50, 150, and 250 ms) were obtained with 2,048 complex data points in *t*<sub>2</sub> (detection period) and 512 points in *t*<sub>1</sub> (evolution period) with a spectral width of 7,508 Hz. Homonuclear 3D NOESY-TOCSY experiments (Oschkinat et al., 1990, 1994) were obtained with 2,048 × 256 × 90 (*F*<sub>3</sub> × *F*<sub>2</sub> × *F*<sub>1</sub>) data points. NMR data were processed on an Indigo II workstation utilizing the UGXNMR (for 2D) and AURELIA (for 3D) software. Experimental restraints (distance and dihedral angle constraints) derived from the NMR experiments were used to calculate the 3D solution structure(s) of CTX V by the random/dynamical simulated annealing using the X-PLOR software (version 3.1; Brünger, 1992). The strategy employed in the structure calculation of CTX V was similar to those used in our earlier structure determination studies (Bhaskaran et al., 1994a, 1994b; Jang et al., 1997; Sivaraman et al., 1998b). The authenticity of the calculated structures were confirmed by backcalculating the NOESY spectrum from the X-PLOR generated 3D structures, using the model utility given in Felix-95 package.

## Acknowledgments

The atomic coordinates of the average solution structure of CTX V have been deposited in the Brookhaven Protein Data Bank (PDB ID-1CHV).

The work was supported by the National Science Council, Taiwan and Dr. C.S. Tsou Memorial Medical Research Advancement Foundation grants. We acknowledge the Regional Instrumentation Centre, Hsinchu, Taiwan for allowing us to use the 600 MHz NMR spectrometer facility.

## References

- Bax A, Davies DG. 1985. MLEV-17 based two-dimensional homonuclear magnetisation transfer spectroscopy. *J Magn Reson* 65:355–360.
- Bhaskaran R, Huang CC, Chang DK, Yu C. 1994a. Cardiotoxins III from the Taiwan cobra (*Naja naja atra*)—Determination of structure in solution and comparison with short neurotoxins. *J Mol Biol* 235:1291–1301.
- Bhaskaran R, Huang CC, Tsai YC, Jayaraman G, Chang DK, Yu C. 1994b. Cardiotoxin II from the Taiwan cobra venom, *Naja naja atra*—Structure in solution and comparison among homologous cardiotoxins. *J Biol Chem* 269:23500–23508.
- Brünger AT. 1992. *X-PLOR software manual*, version 3.1. New Haven, Connecticut: Yale University.
- Carlsson FHH, Louw AJ. 1978. The oxidation of methionine and its effects on the properties of cardiotoxin V<sup>II</sup> from *Naja melanoleuca* venom. *Biochem Biophys Acta* 534:325–329.
- Chang JY, Kumar TKS, Yu C. 1998. Unfolding and refolding of cardiotoxin III elucidated by reversible conversion of the native and scrambled species. *Biochemistry* 37:6745–6751.
- Chiou SH, Hung CC, Huang HC, Chen ST, Wang KT, Yang CC. 1995. Cardiotoxins and cobratoxins isolated from Taiwan cobra. *Biochem Biophys Res Commun* 206:22–32.
- Condrea E. 1974. Membrane active polypeptides from snake venom. Cardiotoxins and hemo cytotoxins. *Experientia* 30:121–129.
- Dufton MJ, Hider RC. 1983. Conformational properties of neurotoxins and cytotoxins isolated from Elapidae snake toxin. *CRC Crit Rev Biochem* 114:113–171.
- Dufton MJ, Hider RC. 1991. The structure and pharmacology of elapid cytotoxins. In: Harvey AL, ed. *Snake toxins*. New York: Pergamon Press. pp 259–302.
- Gantaineau E, Toma F, Montenary-Garester T, Takechi M, Fromageot F, Menez A. 1987. Role of tyrosine and tryptophan residues in the structure-activity relationships of a cardiotoxin from *Naja nigricollis* venom. *Biochemistry* 26:8046–8055.
- Harvey AL. 1985. Cardiotoxins from cobra venom: Possible mechanisms of action. *J Toxicol Toxin Rev* 4:41–69.
- Harvey AL. 1991. Cardiotoxins from snake venoms. In: Tu AT, ed. *Handbook of natural toxins*. New York: Marcel Dekker. pp 85–106.
- Hodges SJ, Agbaji AS, Harvey AL, Hider RC. 1987. Cobra cardiotoxins. Purification, effects on skeletal muscle and structure/activity relationships. *Eur J Biochem* 166:373–383.
- Jahnke W, Mierke DF, Bevers L, Kessler H. 1994. Structure of cobra cardiotoxin CTX I as derived from nuclear magnetic resonance spectroscopy and distance geometry calculations. *J Mol Biol* 240:445–458.
- Jang JY, Kumar TKS, Jayaraman G, Yu C. 1997. Comparison of the hemolytic activity and solution structures of two snake venom cardiotoxin analogues which only differ in their N-terminal amino acid. *Biochemistry* 36:14635–14641.
- Kini RM, Evans HJ. 1989. Role of cationic residues in the cytolytic activity: Modification of lysine residues in the cardiotoxin from *Naja nigricollis* venom and correlation between cytolytic and antiplatelet activity. *Biochemistry* 28:9202–9215.
- Kumar TKS, Jayaraman G, Lee CS, Arunkumar AI, Sivaraman T, Samuel D, Yu C. 1997. Snake venom cardiotoxins—Structure, dynamics, function and folding. *J Biomol Struct Dyn* 15:431–463.
- Kumar TKS, Lee CS, Yu C. 1996a. A case study of cardiotoxin III from the Taiwan cobra (*Naja naja atra*). Solution structure and other physical properties. In: Singh BR, Tu AT, eds. *Natural toxins II*. New York: Plenum Press. pp 115–129.
- Kumar TKS, Pandian SK, Srisailam S, Yu C. 1998. Structure and folding of snake venom cardiotoxins. *J Toxicol Toxin Rev* 17:183–212.
- Kumar TKS, Yang PW, Lin SH, Wu CY, Lei B, Bo SY, Tu SC, Yu C. 1996b. Cloning, direct expression and purification of a snake venom cardiotoxin in *E. coli*. *Biochem Biophys Res Commun* 219:450–456.
- Lee CS, Kumar TKS, Lian LY, Cheng JW, Yu C. 1998. Main chain dynamics of cardiotoxin II from Taiwan cobra (*Naja naja atra*) as studied by carbon-13 NMR at natural abundance: Delineation of the role of functionally important residues. *Biochemistry* 37:155–164.
- Menez A, Botes F, Roumestand C, Gilquin B, Toma F. 1992. Structural basis for functional diversity of animal toxins. *Proc Royal Soc Edinburgh* 90B:83–103.

- Menez A, Gatineau E, Roumestand C, Harvey AL, Mauward L, Gilquin B, Toma F. 1990. Do cardiotoxins possess a functional site? Structural and chemical modification studies reveal the functional site of the cardiotoxin from *Naja nigricollis*. *Biochemie* 72:575–588.
- Oschkinat H, Cieslar C, Griesinger C. 1990. Recognition of secondary structure elements in 3D TOCSY-NOESY spectra of proteins—Interpretation of 3D cross peak amplitudes. *J Magn Reson* 86:453–469.
- Oschkinat H, Muller T, Diechmann T. 1994. Protein structure determination with three-dimensional and four-dimensional NMR spectroscopy. *Angew Chem Int Ed Engl* 33:277–293.
- Piotto M, Saudek V, Skelnar V. 1992. Gradient tailored excitation for single quantum NMR spectroscopy of aqueous solutions. *J Biomol NMR* 2:661–665.
- Rance M, Sorenson OW, Bodenhausen G, Wagner G, Ernst RR, Wuthrich K. 1983. Improved spectral resolution in COSY proton NMR spectra of proteins via double quantum filtering. *Biochim Biophys Res Commun* 117:479–485.
- Rees B, Bilwes A. 1993. Three dimensional structures of neurotoxins and cardiotoxins. *Chem Res Toxicol* 6:385–406.
- Shashidharan P, Ramachandran LK. 1987. Effect of N-bromosuccinimide modification of tyrosine side chains of cardiotoxin II of the Indian cobra on biological activity. *J Biosci* 11:287–297.
- Shiau Lin SY, Huang MC, Lee CY. 1976. Mechanism of action of cobra cardiotoxin on the skeletal muscle. *J Pharmacol Exp Ther* 196:758–770.
- Sivaraman T, Kumar TKS, Chang DK, Lin WY, Yu C. 1998a. Events in the kinetic folding pathway of an all  $\beta$ -sheet protein. *J Biol Chem* 273:10181–10189.
- Sivaraman T, Kumar TKS, Huang CC, Yu C. 1998b. The role of acetic acid in the prevention of aggregation of self-induced aggregation of snake venom cardiotoxins. *Biochem Mol Biol Int* 44:29–39.
- Sivaraman T, Kumar TKS, Yang PW, Yu C. 1997. Cardiotoxin-like basic protein (CLBP) from *Naja naja atra* is not a cardiotoxin. *Toxicon* 35:1367–1371.
- Takechi M, Tanaka Y, Hayashi K. 1985. Cytolytic activity of cytotoxin isolated from Indian cobra venom against experimental tumor cells. *Biochem Int* 11:795–800.
- Takechi M, Tanaka Y, Hayashi K. 1986. Binding of cardiotoxin analogue III from Formosan cobra to FL cells. *FEBS Lett* 205:143–146.
- Thelestam M, Molby R. 1979. Classification of microbial, plant and animal cytotoxins based on their membrane damaging effects on human fibroblasts. *Biochim Biophys Acta* 557:156–169.
- Wuthrich K. 1986. *NMR of proteins and nucleic acids*. New York: John Wiley and Sons.
- Yang CC, King K, Sun TP. 1981. Chemical modification of lysine and histidine residues in phospholipase A2 from the venom of *Naja naja atra*. *Toxicon* 19:645–659.